EXPERIMENTAL STUDY ON THE CO_2 TO WATER HEAT EXCHANGER PERFORMANXCE NEAR THE CO_2 CRITICAL POINT

Yoonhan Ahn, Seongjoon Baik, Jeong Ik Lee

Department of Nuclear and Quantum Engineering, Korea Advanced Institute of Science and Technology 373-1 Guseong-dong Yuseong-gu, Daejeon, 305-701, Korea
Tel: 82-42-350-3829, Fax: 82-42-350-3810
yoonhan.ahn@kaist.ac.kr, bsj227@kaist.ac.kr, jeongiklee@kaist.ac.kr

ABSTRACT

Supercritical CO_2 (S-CO_2) cycle is considered as one of the promising candidates for the next generation nuclear reactor power conversion system due to relatively high efficiency at low turbine inlet temperature. It also has simple layout and small footprint due to compact turbomachinery and heat exchangers. The major characteristic of a S-CO_2 cycle is the small compression work due to dynamic thermodynamic property variation near the critical point. As the S-CO_2 cycle efficiency is highly dependent on the compressor inlet condition, the performance of precooler must be investigated thoroughly as the precooler conditions the compressor inlet condition. For such application, conventional shell and tube heat exchanger can be considered. To investigate the CO_2 heat transfer near the critical point to the water acting as the ultimate heat sink, the experimental data obtained from S-CO_2 Pressurizing Experiment (SCO_2PE) were utilized. SCO_2PE is composed of a canned motor type CO_2 compressor, an expansion valve and a spiral tube heat exchanger. The conventional LMTD method was utilized for the spiral tube heat exchanger design evaluation. However, the heat exchanger performance differs from the design point as the CO_2 specific heat changes vigorously near the critical point. To assess the CO_2 heat transfer more precisely, the average Nusselt number is calculated and compared with the existing correlations.

KEYWORDS
Supercritical CO_2, heat transfer, critical point, LMTD method, average Nusselt number

1. INTRODUCTION

As the concern for the global climate change is gradually increasing, the nuclear energy is considered as one of the realistic alternative to reduce the CO_2 emission. Among the next generation nuclear reactor designs, the Sodium-cooled Fast Reactor (SFR) has been actively researched with abundant operating experience in several leading countries. Recently, 150MW_e Prototype Generation IV Sodium-cooled Fast Reactor (PG-SFR) is being developed by the Korean Atomic Energy Research Institute (KAERI). The current design of PG-SFR adopts a superheated steam Rankine cycle for its power conversion system. However, a possibility of having violent sodium-water reaction in SFR requires a safety system such as a double wall steam generator or a waveguide sensor visualization technology to mitigate the consequences from an accident. To prevent the sodium-water reaction inherently, a Supercritical CO_2 (S-CO_2) cycle is considered as the promising alternative to replace the sodium water reaction with the mild sodium-CO_2 reaction.

A S-CO_2 cycle is receiving attention as an alternative to the steam Rankine cycle due to the benefits summarized below.

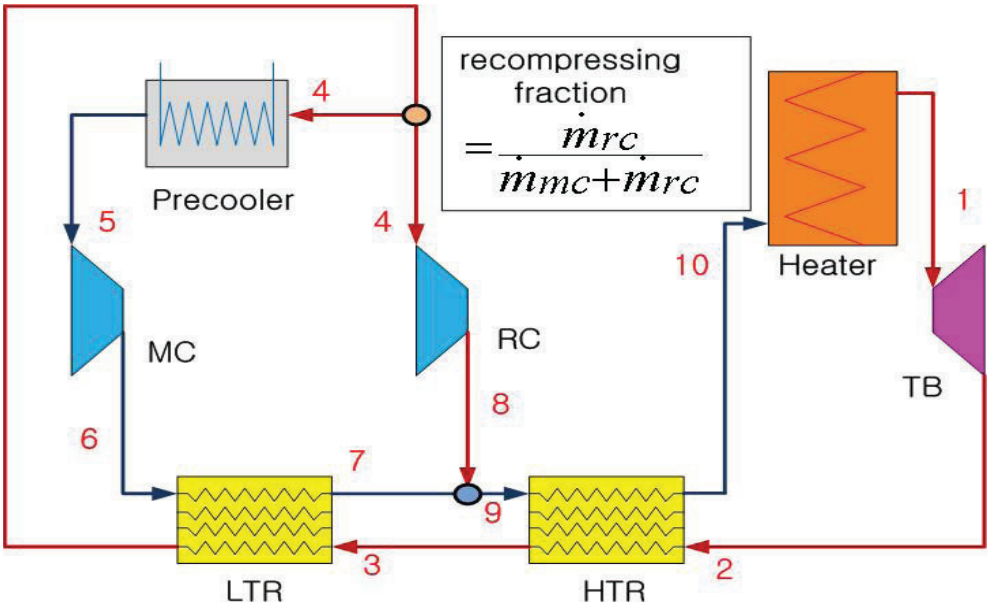

Figure 1. S-CO_2 Recompression cycle layout

- Competitive efficiency under low turbine inlet temperature
- Simple layout to achieve high efficiency
- Small footprint with compact turbomachinery and heat exchangers
- Less complexity in purification system requirements compared to the steam Rankine cycle

As shown in Figure 1, a S-CO_2 recompression cycle is considered as one of the most efficient layouts. Previous studies showed that the S-CO_2 cycle efficiency is highly sensitive to the compressor inlet condition which is close to the critical point (30.98^{o}C, 7.3773MPa) [1]. Therefore, evaluation of the main compressor as well as the precooler performances are essential for realizing the S-CO_2 cycle design. Among various types of heat exchanger, the Printed Circuit Heat Exchanger (PCHE) has been widely utilized for the S-CO_2 cycle due to a wide range of operational temperature and pressure. In general, operating conditions of recuperators and CO_2 heaters in the cycle are usually appropriate for PCHE due to high pressure difference between hot and cold fluids. However, several alternative heat exchangers including Shell and tube type Heat Exchanger (SHE) has been investigated due to relatively low pressure difference in the precooler. The heat transfer analysis results for water to CO_2 in the precooler under the condition of largely varying CO_2 thermodynamic properties are presented in this paper.

2. Supercritical CO_2 Pressurizing Experiment (SCO_2PE) and experiment data

2.1. SCO_2PE and Spiral Tube Heat Exchanger (STHE) description

To investigate the CO_2 flow and heat transfer characteristics near the critical point, the Supercritical CO_2 Pressurizing Equipment (SCO_2PE) was designed and constructed by KAIST research team. As shown in Figure 2, SCO_2PE consists of a low pressure ratio canned motor type CO_2 compressor, an expansion valve, an electric heater, and a Spiral Tube Heat Exchanger (STHE). In addition, the booster pump and venting valve were installed to charge and vent CO_2,

respectively. In the cooling water tank, the chiller is connected to cool water. The measurement devices are installed to measure the inlet and outlet condition of STHE and CO_2 compressor.

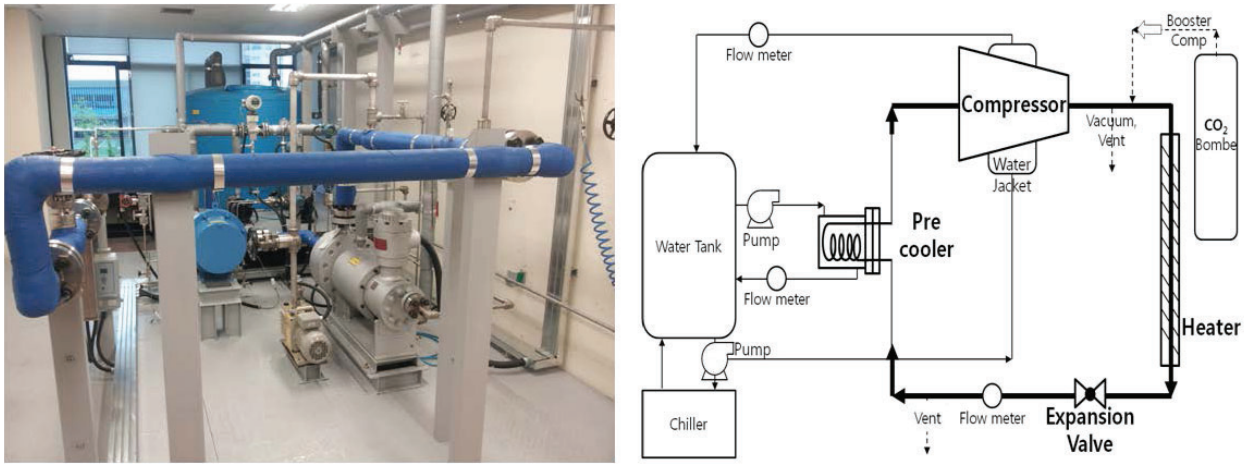

Figure 2. SCO_2PE picture (left) and schematic layout (right)

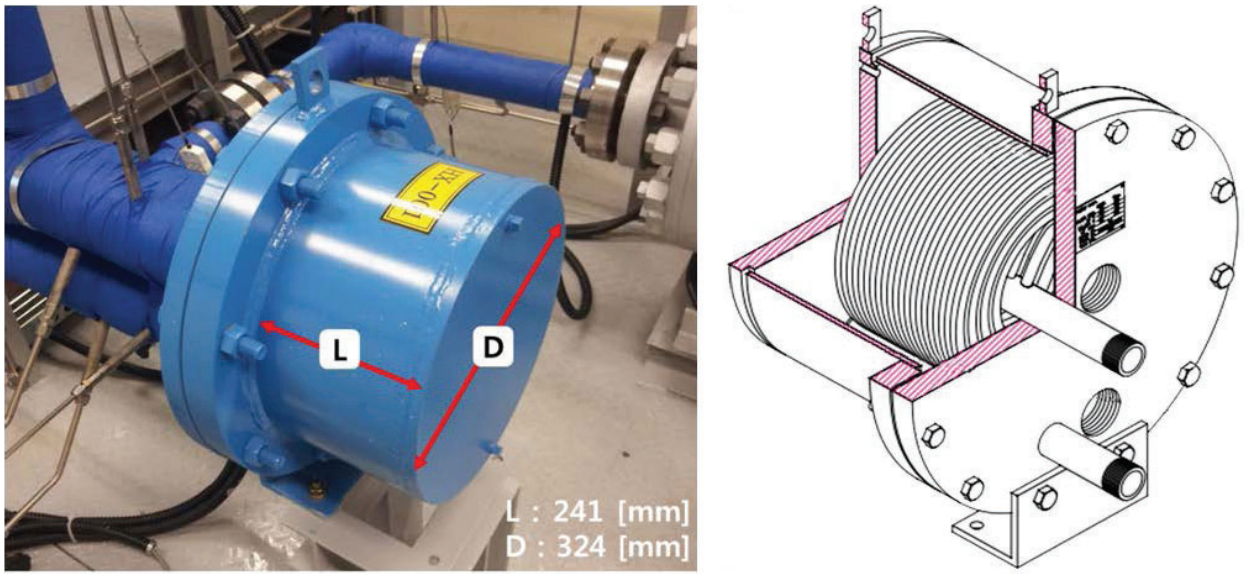

Figure 3. Spiral Tube Heat Exchanger (STHE) type precooler (courtesy of Sentry Equipment Corp.)

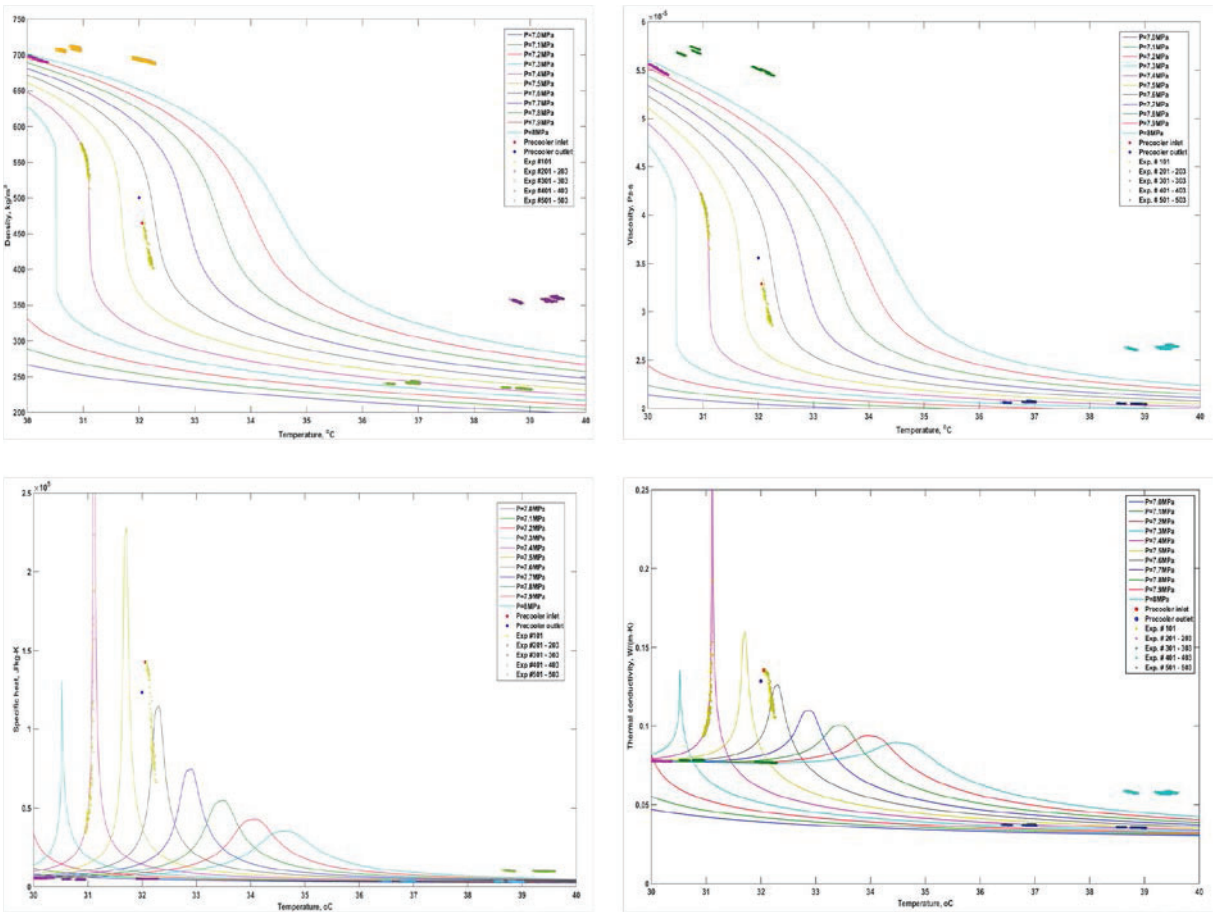

Figure 4. CO_2 properties (density, viscosity, specific heat, thermal conductivity) variation near the critical point region

The experimental procedure of SCO_2PE is as below.
- After vacuuming with a vacuum pump, CO_2 in a tank is transported to the main loop with the booster pump.
- While charging CO_2, the mass in the loop is monitored and heated to the supercritical state through an electric heater.
- Supercritical CO_2 is compressed with the compressor and expanded through an expansion valve. Then, CO_2 is cooled near to the critical point in the precooler.

The picture and the internal geometry of the STHE is shown in Figure 3. Water in the shell side is pumped from the cooling water tank which cools the high pressure CO_2 in the tube side flowing near the critical point. As shown in Figure 4, the properties vary dramatically near the critical point. Several design parameters are listed in Table I. Due to the limited information from the manufacturing company, some parameters are assumed based on the heat exchanger geometry.

Table I. Spiral Tube Heat Exchanger (STHE) design parameters

	Tube (CO_2)	Shell (water)	Correction factor, F	0.314
Design T_{in}, ^oC	32.06	7	Heat load, kW	23.41
Design T_{out}, ^oC	32	12.3	Heat transfer area, m^2	2.022
Mass flow rate, kg/s	2.78	1.05	N_{tube}	20

Reference viscosity, cp	0.03421	1.307	ID_{tube}, m	0.00775
Reference density, kg/s	482.62	1000	OD_{tube}, m	0.00953
Reference thermal conductivity, W/m-K	0.1341	0.58684	L_{tube}, m	1.17
Reference specific heat, kJ/kg-K	140.34	4.19	Tube thermal conductivity, W/m-K	16.2
Reference Pr	35.8	9.34	Tube material	SS316
Log mean temperature difference, ΔT_{lm}	22.27		Overall heat transfer coefficeint, W/m^2-K	1656.4
OD_{shell}	0.324		L_{shell}	0.241

Based on the LMTD methods, the heat transfer rates from the hot fluid to cold fluid in the heat exchanger can be expressed as below, respectively.

$$q = UAF\Delta T_{lm} \tag{1}$$

F is log-mean temperature difference correction factor. This dimensionless parameter is dependent on the number of transfer unit (NTU), the flow configuration and the heat capacity ratio between hot and cold side. From the design parameters provided from the manufacturing company, the corresponding value of F is calculated and shown in Table I.

2.2. Experiment data and uncertainty analysis

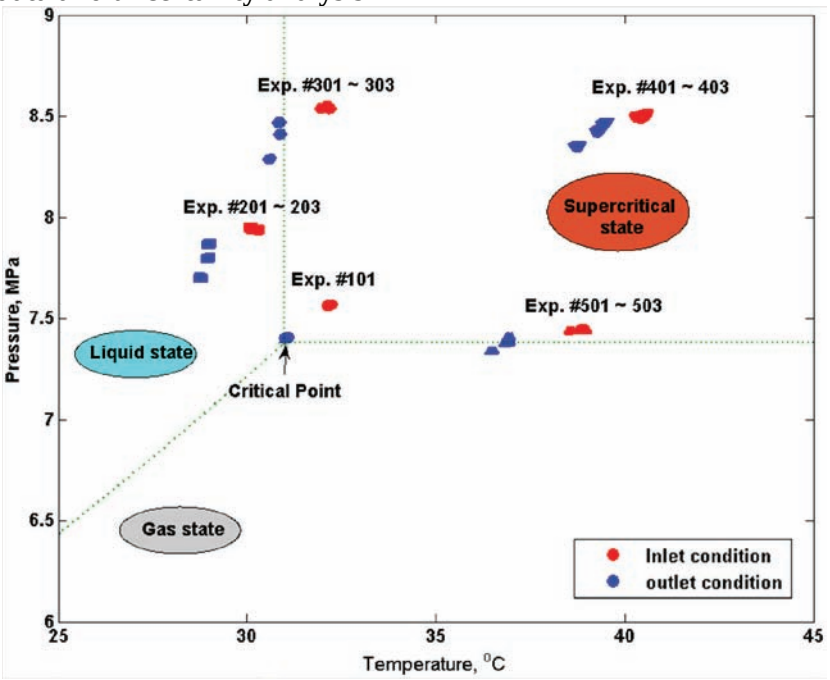

Figure 5. Experiment data case

Table II. Experiment data

Exp. No	$\dot{m}_{tube}$, kg/s	$T_{in,\ tube}$, °C	$P_{in,\ tube}$, MPa	$T_{out,\ tube}$, °C	$P_{in,\ tube}$, MPa	$\dot{m}_{shell}$, kg/s	$T_{in,\ shell}$, °C	$T_{out,\ shell}$, °C	ΔP_{shell}, kPa
101	2.74	32.17	7.566	31.04	7.403	0.19	6.89	28.25	145
201	4.00	28.91	7.949	28.78	7.699	0.27	15.13	26.91	236
202	2.98	29.14	7.938	28.99	7.796	0.23	14.94	27.16	189

203	2.02	29.20	7.934	29.01	7.868	0.20	14.86	27.37	155
301	3.97	30.76	8.538	30.62	8.288	0.23	14.98	28.70	189
302	2.97	31.05	8.551	30.88	8.410	0.20	15.06	29.09	149
303	2.02	31.06	8.538	30.87	8.470	0.17	14.78	29.22	107
401	2.15	38.87	8.498	38.78	8.352	0.08	14.86	38.26	32
402	1.54	39.51	8.504	39.33	8.428	0.06	15.09	38.79	28
403	0.98	39.72	8.498	39.49	8.466	0.05	14.92	39.15	26
501	0.84	37.14	7.438	36.94	7.404	0.05	15.10	37.34	33
502	1.20	37.02	7.444	36.90	7.375	0.06	14.99	37.00	28
503	1.45	36.60	7.436	36.51	7.337	0.07	15.10	36.51	29

Table III. Measurement accuracy

Sensor type	Accuracy
RTD	$+0.2^{o}$C
Pressure transmitter	± 0.05%
Differential pressure gauge (CO_2)	± 0.065%
Differential pressure gauge (water)	± 0.04%
Mass flow meter (CO_2)	± 0.16%
Mass flow meter (water)	± 0.5%

Several experiment data from SCO_2PE were acquired and shown in Fig. 5 and Table II. The heat exchanging experiments were conducted in various conditions including below and over the critical point. Before evaluating heat transfer rate from the experimental data, the uncertainty analysis was performed. Due to the nonlinear property change of CO_2 near the critical point, the measurement uncertainties can influence the heat transfer analysis. The measurement device type and accuracy are listed in Table III. The uncertainties of enthalpy, transferred heat, Reynolds number and Prandtl number can be derived as below [3].

$$\frac{\omega_h}{h} = \sqrt{(\frac{\delta h}{\delta T}\omega_T)^2 + (\frac{\delta h}{\delta P}\omega_P)^2} \tag{2}$$

$$\frac{\omega_Q}{Q} = \sqrt{(\frac{\omega_{\dot{m}}}{\dot{m}})^2 + (\frac{\omega_{h_{in}}}{h_{in}})^2 + (\frac{\omega_{h_{out}}}{h_{out}})^2} \tag{3}$$

$$\frac{\omega_{\mathrm{Re}}}{\mathrm{Re}} = \sqrt{(\frac{\omega_{\dot{m}}}{\dot{m}})^2 + (\frac{\omega_\mu}{\mu})^2} \tag{4}$$

$$\frac{\omega_{\mathrm{Pr}}}{\mathrm{Pr}} = \sqrt{(\frac{\omega_k}{k})^2 + (\frac{\omega_{c_p}}{c_p})^2 + (\frac{\omega_\mu}{\mu})^2} \tag{5}$$

Table IV. Enthalpy and heat uncertainty analysis

	$(\frac{\omega_h}{h})_{co_2}$	$(\frac{\omega_h}{h})_{water}$	$(\frac{\omega_Q}{Q})_{co_2}$	$(\frac{\omega_Q}{Q})_{water}$	$(\frac{\omega_{\mathrm{Re}}}{\mathrm{Re}})_{CO_2}$	$(\frac{\omega_{\mathrm{Pr}}}{\mathrm{Pr}})_{CO_2}$
Exp. #101	2.24 - 58.29	0.7 - 2.97	4.83 - 58.29	2.94 - 3.1	9.9 - 25.3	26.8 - 134.8
Exp. #201 - 203	0.35 - 0.4	0.73 - 1.33	0.55 - 0.56	1.59 - 1.62	1.0	3.0 - 3.4
Exp. #301 - 303	0.33 - 0.36	0.68 - 1.35	0.51 - 0.52	1.57 - 1.60	0.9	2.4 - 2.6
Exp. #401 - 403	0.41 - 0.56	0.51 - 1.34	0.69 - 0.72	1.50 - 1.53	0.9	4.8 - 5.3
Exp. #501 - 503	0.17 - 0.2	0.53 - 1.33	0.3 - 0.31	1.50 - 1.53	0.2	1.7 - 1.9

(unit : %)

Table IV clearly shows that the uncertainty of parameters such as enthalpy, transferred heat, Reynolds number and Prandtl number near the CO_2 critical point is distinctively higher than other cases. Except for Exp. #101, the uncertainties are comparably reasonably low although the operating conditions are still near the critical point. Among the accumulated experiment cases, the uncertainties of Exp. 501 - 503 are the lowest.

2.3. Heat transfer analysis

Based on equation (2), the overall heat transfer coefficient can be calculated from the experiment data with the value of heat transfer area and log mean temperature difference. The heat is transferred from CO_2 to the hot wall through convection, conduction through the tube wall and convection from the tube wall to the shell side water. If the fouling factor is ignored, the overall heat transfer coefficient, U can be expressed as below.

$$\frac{1}{U} = \frac{1}{h_o} + \frac{d_o \ln(d_o / d_i)}{2k_w} + \frac{d_o}{h_i d_i} \tag{6}$$

where h_o, h_i, d_o, d_i, and k_w are tube outside heat transfer coefficient, tube inside heat transfer coefficient, tube outer diameter, tube inner diameter and wall thermal conductivity, respectively. For the analysis of heat transfer in a pipe is quite straight forward. The average Nusselt number is calculated from Gnielinski correlation [4]. The Reynolds number of CO_2 varies from 413,000 - 30,000,000 and the fluid can be regarded as turbulent.

$$Nu = \frac{(f/8)(\mathrm{Re}-1000)\,\mathrm{Pr}}{1.00 + 12.7(f/8)^{1/2}(\mathrm{Pr}^{2/3}-1)} \tag{7}$$

$$f = \frac{1}{(1.82\log_{10}\mathrm{Re} - 1.64)^2} \tag{8}$$

where $2{,}300 < \mathrm{Re} < 5 \times 10^6$ and $1.0 < \mathrm{Pr} < 10^6$.
However, the heat transfer in a shell needs more consideration to simplify the complicated shell geometry. To calculate the Reynolds number of water flow, the fluid velocity and the hydraulic diameter must be determined. To calculate the fluid velocity, the cross sectional area was simplified as below.

$$A_{cx,shell} = (V_{shell} - V_{tube}) / L_{shell} \tag{9}$$

where $A_{cx,shell}$, V_{shell}, V_{tube} and L_{shell} are shell side cross sectional area, shell side volume, tube side volume and shell side length, respectively. The water velocity in the shell is quite low as the cross sectional area is large. The Reynolds number of water flow varies from 290 - 380. The cross flow in the shell with the staggered tubes is calculated with the following correlation [5].

$$Nu = 0.71 \mathrm{Re}^{0.5} \mathrm{Pr}^{0.36} \quad (10)$$

where the correlation is valid for 100 <Re< 1000.
From this analysis, the overall heat transfer coefficient is calculated and compared with the experiment data as shown in Figure 6. In general, the calculated overall heat transfer coefficient, U_{cal} is higher than the experiment data.

Table V. Thermal resistance analysis

	Heat, kW	U_{cal}, kW/m^2-K	$\frac{R_{shell}}{U}$, %	$\frac{R_{tube}}{U}$, %	$\frac{R_{wall}}{U}$, %
Case #101	16.93- 17.53	2.36 - 2.41	82.4 - 83.4	2.2 - 3.3	14.3 - 14.6
Case #201 - 203	10.34- 13.78	2.12 - 2.30	68.7 - 71.9	12.4 - 18.3	12.9 - 15.8
Case #301 - 303	10.14- 13.82	1.99 - 2.44	69.9 - 73.1	12.1 - 17.9	12.1 - 14.8
Case #401 - 403	5.14- 7.9	1.21 - 1.58	77.1 - 81.3	9.3 - 15.3	7.3 - 9.6
Case #501 - 503	4.89- 6.05	1.07 - 1.30	66.6 - 73.3	19.1 - 26.8	6.5 - 7.9

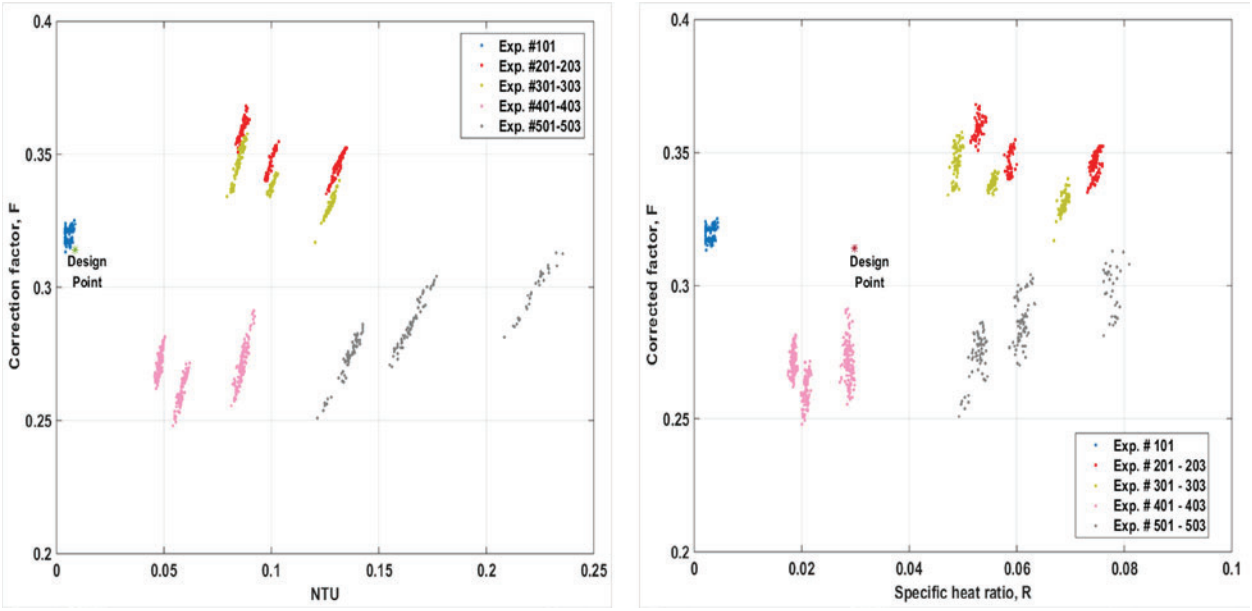

Figure 6. Correction factor from the experiment cases

Table VI. Correction factor analysis

	NTU_{tube}	R_{tube}	$F_{correction}$
Case #101	0.0039 - 0.0086	0.0021 - 0.0045	0.313 - 0.325
Case #201 - 203	0.0835 - 0.1349	0.0515 - 0.0760	0.335 - 0.368
Case #301 - 303	0.0795 - 0.1318	0.0472 - 0.0698	0.317 - 0.358
Case #401 - 403	0.0456 - 0.0921	0.0175 - 0.0300	0.248 - 0.291
Case #501 - 503	0.1215 - 0.2354	0.0493 - 0.0810	0.251 - 0.313

$$NTU = \frac{UA}{C} = \frac{UA}{(\dot{m} c_p)} \tag{11}$$

$$R_{tube} = \frac{C_{shell}}{C_{tube}} \tag{12}$$

The thermal resistances of test cases are listed in Table V and the largest thermal resistance was observed from the shell side. While the inlet temperature and pressure were maintained for each test group (e.g. Case#201 - 203), the mass flow rate of tube and shell sides were varied. Consequently, the amount of transferred heat in each case varied when the mass flow rate was varied.

The correction factor of experiments is shown in Table VI. The correction factor is dependent on the number of heat transfer (NTU), the flow configuration and the heat capacity ratio between hot and cold streams (R). For a heat exchanger with well-defined geometry such as counter current flow or parallel flow, the correction factor for the corresponding condition is evaluated. However, the correction factor of a complex geometry heat exchanger cannot not be evaluated. As shown in the left of Figure 6, the calculated correction factor is close to the design point under the similar number of transfer unit (NTU) condition. Based on the open literature correlation, the correction factor is calculated to be in between 0.25 - 0.4.

CONCLUSIONS

Among S-CO_2 heat exchangers in the S-CO_2 cycle, the precooler operating pressure is the lowest compared to other type of heat exchangers and the hot and cold side pressure difference is the lowest. A Printed Circuit Heat Exchanger (PCHE) has been widely utilized for the S-CO_2 heat exchangers but high cost of PCHE can limit the S-CO_2 cycle application. Therefore, an alternative to PCHE for the S-CO_2 cycle is being investigated. A Spiral Tube Heat Exchanger (STHE) is installed in the S-CO_2 Pressurizing Experiment (SCO_2PE) and the preliminary test results were obtained to assess STHE for the precooler performance. From the experiments, thermal resistance of water is larger than that of CO_2. If the shell and tube heat exchanger is utilized for the precooler of S-CO_2 cycle, the heat transfer of shell side must be precisely modeled for the better design and performance prediction.

The design and performance of a Spiral Tube Heat Exchanger were investigated with LMTD method. Based on the design and geometry parameters of STHE, the heat transfer rate was calculated and compared to the experiment data in various cases. From the overall heat transfer rate difference between the experiment data and calculated value, the correction factor was calculated for several different conditions. The correction factor from the experiments varies between 0.25 to 0.4.

ACKNOWLEDGMENTS

Authors gratefully acknowledge that this research is supported by the National Research Foundation of Korea(NRF) and funded by the Korean Ministry of Science, ICT and Future Planning.

REFERENCES

1. W. S. Jeong, Improvement of Supercritical CO2 Brayton Cycle Using Binary Gas Mixture, Master thesis, KAIST, 2011
2. S. G. Kim, J. Lee, Y. Ahn, J. I. Lee, Y. Addad, B. Ko, CFD investigation of a centrifugal compressor derived from pump technology for supercritical carbon dioxide as a working fluid, The Journal of Supercritical Fluids, Vol. 86, 160-171, 2014
3. J. P. Holman, Experimental Methods for Engineers, McGraw-Hill, New York, NY, USA, 2011
4. Ramesh K. Shah, Dusan P. Sekulic, Fundamentals of heat exchanger design, Chapter3., Wiley, John Wiley & Sons, Inc., USA. 2002
5. Adrian Bejan, Allan D. Kraus, Heat transfer handbook, Chapter 6., Wiley, John Wiley & Sons, Inc., USA. 2002